Chinese Chemical Letters 31 (2020) 869–874

Contents lists available at ScienceDirect

Chinese Chemical Letters

journal homepage: www.elsevier.com/locate/cclet

Communication

All-small-molecule dynamic covalent gels with antibacterial activity by boronate-tannic acid gelation

Xuejing Cheng[a], Mengyu Li[a], Hui Wang[b,*], Yiyun Cheng[a,b,**]

[a] Shanghai Key Laboratory of Regulatory Biology, School of Life Sciences, East China Normal University, Shanghai 200241, China
[b] South China Advanced Institute for Soft Matter Science and Technology, South China University of Technology, Guangzhou 510640, China

ARTICLE INFO

Article history:
Received 6 June 2019
Received in revised form 29 June 2019
Accepted 4 July 2019
Available online 4 July 2019

Keywords:
Nature polyphenols
Boronic acids
Hydrogels
Boronate-catechol complexation
All-small-molecule dynamic covalent gels

ABSTRACT

Reversible boronate-catechol linkage was widely used to construct two-dimensional coatings and three-dimensional nanostructures or hydrogels. The construction of these functional materials usually requires the pre-synthesis of macromolecular building blocks, and direct gelation between natural polyphenols and small molecule boronic acids is yet to be investigated. In this study, we fabricated a family of all-small-molecule dynamic covalent gels consisting of tannic acid and boronic acids. Transparent and thixotropic gels were formed by boronate affinity towards catechol groups abundant on natural polyphenols. The gels showed multi-responsiveness, such as acid-, base-, reduction- and oxidant-sensitive depending on the used boronic acid building blocks. The chemistry for gel formation and stimuli-responsiveness was characterized by ^{11}B NMR spectroscopy. The multi-stimuli responsiveness, green processing and facile modular design make the boronic acid-tannic acid gels promising candidates for the development of smart soft materials.

Stimuli-responsive gels are intriguing materials for various applications ranging from flexible electronics, artificial muscles, actuators, and sensors to the mimicry of extracellular matrix for cell culture and tissue regeneration [1,2]. These applications usually require the gels to exhibit responsiveness to multiple triggers such as acid/base, redox signals, enzymes, heat, and light [3–5]. The early generation of responsive gels is designed based on the inherent property of used polymers, *i.e.*, temperature-sensitive poly(*N*-isopropyl acrylamide) and pH-sensitive poly(acrylic acid). To expand the stimuli-responsiveness of the gels, dynamic covalent linkages such as boronate esters, disulfide bonds, thioesters, hemiaminal, and imine bonds or reversible non-covalent host-guest pairs such as cyclodextrin/azobenzene were introduced to form polymer networks [6–11]. These gels could respond to various stimuli by specific material design, but usually require the pre-synthesis of macromolecular building blocks with chemical reactive ligands on the backbone or side chains. This involves high complexity in material synthesis, which limits the large scale and repeatable preparation of corresponding gels [12].

An alternative strategy is synthesis of low molecular weight gelators containing dynamic covalent connections that can form fibrous networks *via* supramolecular assembly [13–17]. These supramolecular gels can be facilely prepared, but usually only respond to a single or two stimuli. In addition, the non-covalent forces holding the supramolecular gel are relatively weak, and this may lead to low gel stability [18]. It is hypothesized that dynamic covalent linkages can be used to directly crosslink small molecules with multiple functional groups [19,20], yielding a class of all-small-molecule dynamic covalent gels. Here, we report the preparation of such gels by direct gelation of natural occurring polyphenol tannic acid (TA) with a series of commercially available inorganic borate (1–4) or organic boronate (5–6) building blocks *via* reversible boronate ester bonds. Though the boronate esters with catechol, 1,2 or 1,3 diols were widely used as reversible linkages in responsive polymeric gels [21–26], the direct gelation of naturally occurring small molecules using this dynamic covalent chemistry is yet to be investigated. The formed gels are responsive to acid/base, oxidants or reducing chemicals depending on the chosen borate/boronate building blocks.

TA is a natural occurring hydrophilic polyphenol with a high density of pyrogallic acid or catechol groups on its structure. Its excellent aqueous solubility and multiple reactive catechol groups make it an ideal candidate in the preparation of all-small-molecule dynamic covalent hydrogels [27–30]. Here, commercially available inorganic borates including $NaBO_2$, $Na_2B_4O_7$, Na_2BO_3 and H_3BO_3/

* Corresponding author.
** Corresponding author at: Shanghai Key Laboratory of Regulatory Biology, School of Life Sciences, East China Normal University, Shanghai 200241, China.
E-mail addresses: wangh@scut.edu.cn (H. Wang), yycheng@mail.ustc.edu.cn (Y. Cheng).

https://doi.org/10.1016/j.cclet.2019.07.013
1001-8417/

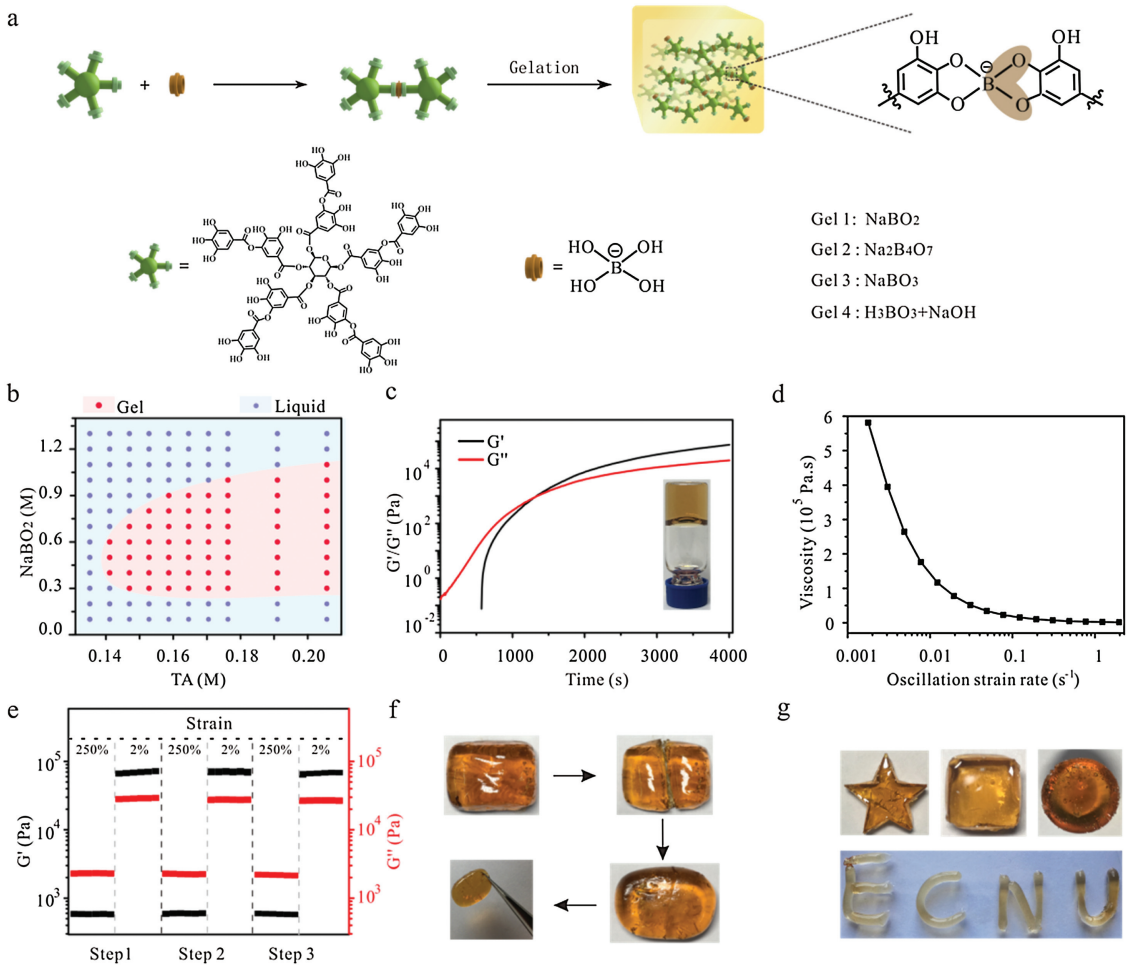

Fig. 1. TA/borate hydrogels. (a) Formation of TA/borate hydrogels by dynamic covalent connections between TA and several inorganic borates (Gel 1, $NaBO_2$; Gel 2, $Na_2B_4O_7$; Gel 3, $NaBO_3$; Gel 4, H_3BO_3 and NaOH). (b) Phase diagram of TA/$NaBO_2$ mixtures. Time-dependent rheology (c), shear-thinning (d) and thixotropic (e) properties of the TA/$NaBO_2$ hydrogel (Gel 1). (f) Self-healing behavior of Gel 1. (g) Gel 1 was fabricated into different shapes.

NaOH were firstly used to crosslink the TA molecules in aqueous solution *via* boronate ester bonds (Fig. 1a). Take $NaBO_2$ for example, the inorganic borate could form hydrogels with TA within a wide concentration ranges for both $NaBO_2$ and TA (Fig. 1b). A yellow-colored and transparent hydrogel (Gel 1) was formed within minutes by gently mixing the two solutions together at ambient temperature. Rheology result in Fig. 1c showed that the storage modulus (G') of a representative gel is higher than the loss modulus (G") after 1200 s, which is usually considered as the gelation time. We then investigated the effects of $NaBO_2$ and TA concentrations on the gel stiffness and gelation time (Figs. S1a-d in Supporting information). When the $NaBO_2$ concentration increased from 0.3 mol/L to 0.4 mol/L, the storage modulus of hydrogel increased and the gelation time decreased. With a further increase in $NaBO_2$ concentration, a reverse trend was observed. Assuming there are five binding sites on each TA molecule, 0.4 mol/L $NaBO_2$ is theoretically to interact with 0.16 mol/L TA *via* the formation of catechol-borate diesters. Therefore, a maximum storage modulus and shortest gelation time were achieved at 0.4 mol/L $NaBO_2$. More borates in the system will lead to increased catechol-borate monoesters, and decreased crosslinking degree in the gel. On the other hand, when the TA concentration was increased from 0.13 mol/L to 0.22 mol/L, the storage modulus increased, while the gelation time decreased. This is due to increased content of catechol-borate diesters and hydrogen bonding interactions in the network at higher TA concentrations. Like most hydrogels, the yielding TA/$NaBO_2$ gel displayed shear-thinning (Fig. 1d), thixotropic (Fig. 1e), self-healing (Fig. 1f) properties, and could be processed to different shapes using specific molds (Fig. 1g).

We next investigated the mechanism of TA/$NaBO_2$ gelation in aqueous solution by solution ^{11}B NMR spectroscopy. The samples were prepared at TA to $NaBO_2$ molar ratios ranging from 0:1 to 0.26:1 in deuterated water at pH 5.5 (no gelation observed under this condition, pH 5.5 is the pH value for TA/$NaBO_2$ mixture in Gel 1), and added into Teflon tubes for ^{11}B NMR measurement. As shown in Fig. 2a, $NaBO_2$ alone showed a sharp peak at 20.1 ppm at pH 5.5, which is the characteristic peak for tetrahedral borate anion [31]. After the addition of TA molecules, a new peak at 8.7 ppm was observed, and this peak is assigned to the borate monoester formed between catechol and tetrahedral borate anion. With increasing molar ratio of TA to $NaBO_2$, the intensity for the peak at 8.7 ppm is increased, and another peak at 14.7 ppm assigned to the borate diesters is observed. The chemical shifts for catechol-borate monoesters and diesters are in accordance with the reference results [31,32]. The catechol-borate diesters are the major driven force for gelation between TA and tetrahedral borate (Fig. 2b). Besides ^{11}B NMR, we also characterized the TA/$NaBO_2$ gel by a resonance Raman Spectroscopy. Compared to free TA or

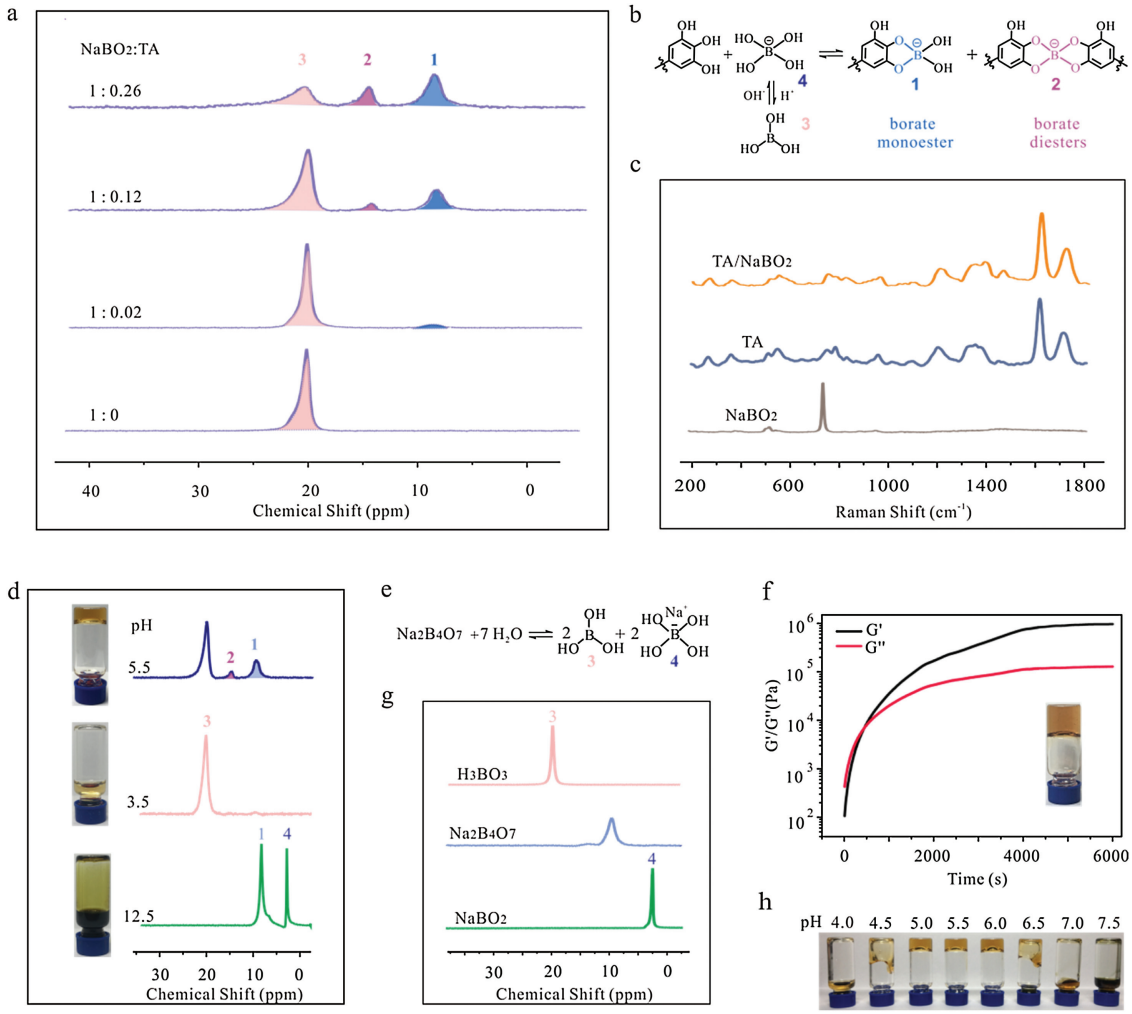

Fig. 2. Gelation and degradation mechanisms of the TA/borates hydrogels. (a) Solution ^{11}B NMR spectra of TA/$NaBO_2$ mixtures. The TA to $NaBO_2$ molar ratios were ranged from 0:1 to 0.26:1 in D_2O fixed at pH 5.5. (b) The formation of catechol-borate monoesters and diesters between TA and $NaBO_2$. (c) Raman spectra of TA, $NaBO_2$, and TA/$NaBO_2$ hydrogels. (d) ^{11}B NMR spectra of TA/$NaBO_2$ in D_2O at a molar ratio of 1:0.12 at different pH conditions. (e) The hydrolysis of $Na_2B_4O_7$ in aqueous solution. (f) Time-dependent rheology of the TA/$Na_2B_4O_7$ hydrogel (Gel 2). (g) ^{11}B NMR spectra of $NaBO_2$, $Na_2B_4O_7$, H_3BO_3 in D_2O. (h) TA/$Na_2B_4O_7$ mixtures at various pH conditions.

$NaBO_2$, a new peak was observed at 1412 cm^{-1} which is assigned to catechol-borate esters in the formed gels (Fig. 2c). The responsive behaviors of Gel 1 to acid or base were then investigated. As shown in Fig. 2d and Fig. S2 (Supporting information), the formed TA/$NaBO_2$ gel was relatively stable at pH 5.0–6.0, but rapidly dissolved in the presence of HCl or NaOH. This can be explained by the cleavage of catechol-borate diesters in acidic environments and hydrolysis/oxidation of TA in basic conditions [33–35]. These speculations were confirmed by ^{11}B NMR results in Fig. 2d, where the catechol-borate diesters were disappeared in both cases.

According to the analysis above, tetrahedral borate is the key structure for TA/borate gelation. Therefore, other inorganic borates that could hydrolyze into tetrahedral borate have the potential of gelation with TA *via* the dynamic covalent chemistry. $Na_2B_4O_7$ is a naturally occurring inorganic borate can be hydrolyzed to trigonal and tetrahedral borates at an appropriate molar ratio of 1:1 in aqueous solution (Fig. 2e). As shown in Fig. 2f, TA and $Na_2B_4O_7$ also form a transparent and yellow-colored gel after gentle mixing (Gel 2). In the ^{11}B NMR spectrum (Fig. 2g), a peak of 9.7 ppm is observed in the $Na_2B_4O_7$ solution (0.4 mol/L, pH 9.3), this peak is the weighted average of trigonal-state (2.5 ppm) and tetrahedral-state (20.1 ppm) borates in solution, which exhibiting a fast exchange between the two states within the NMR time scale [31]. The content of tetrahedral borates in the $Na_2B_4O_7$ solution can be modulated by facilely changing the solution pH, and this property can be used to tune the gel state. As shown in Fig. 2h, the TA/$Na_2B_4O_7$ hydrogel is also pH-responsive and stable TA/$Na_2B_4O_7$ gels were formed within the pH range of 5.0-6.0. Besides $Na_2B_4O_7$, $NaBO_3$ and a mixture of H_3BO_3 and NaOH at a molar ratio of 1:1 can be used to prepare dynamic covalent hydrogels with TA (Gel 3 and Gel 4, Fig. S3 in Supporting information).

TA has been widely reported with antibacterial activity by destabilizing the bacteria membrane [36]. We further investigated the *in vitro* antibacterial activity of the prepared hydrogels. As shown in Figs. 3a and b, the natural polyphenol TA and all the TA/borate hydrogels effectively inhibited the growth of *E. coli*, suggesting the potent antibacterial activity of TA and TA-containing gels. The borates $NaBO_2$ and $Na_2B_4O_7$ showed limited effect on the inhibition of *E. coli* growth. Interestingly, $NaBO_3$ effectively killed the bacteria at an equal borate concentration. This

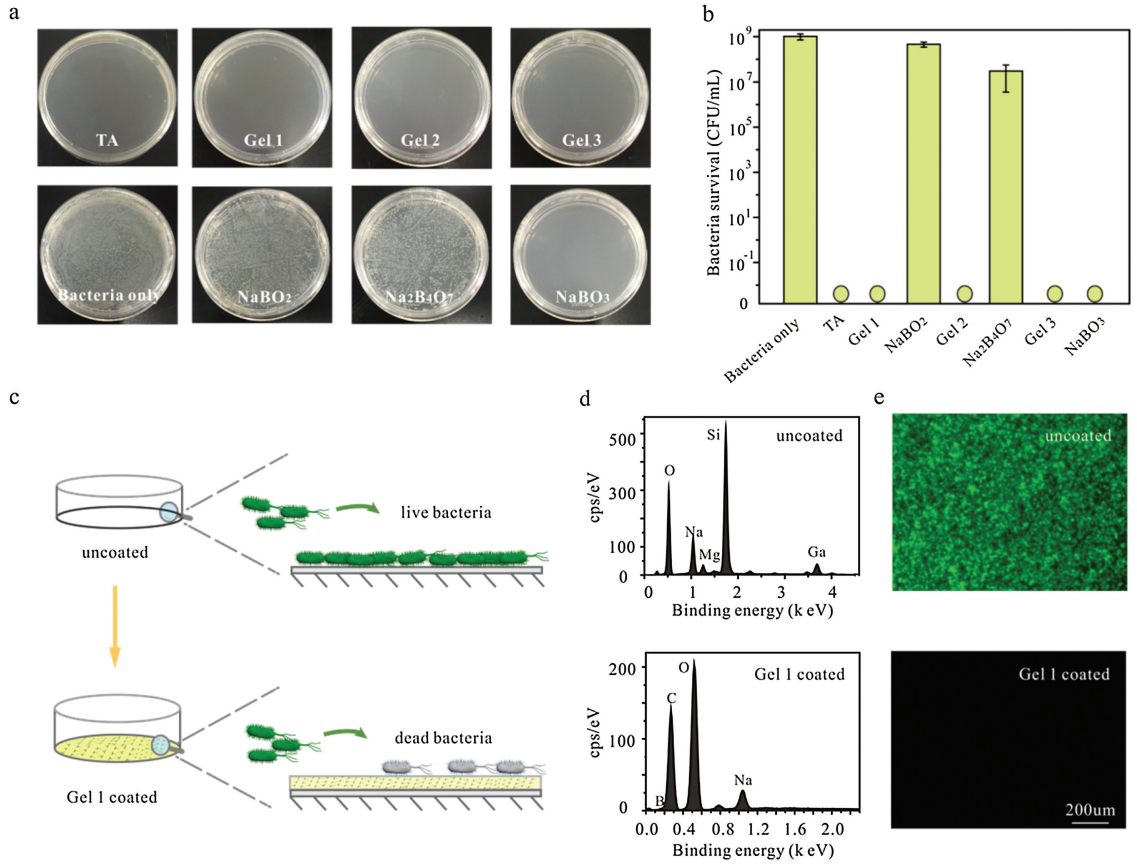

Fig. 3. (a) Images of LB agar inoculated with *E. coli* suspensions incubated on TA/borate hydrogel-coated plates (Gel 1-Gel 3). TA, $NaBO_2$, $Na_2B_4O_7$ and $NaBO_3$ were tested as controls. The white dots on the plates are live bacteria colonies. (b) Antibacterial activities of the hydrogels and chemicals in (a). (c) Coating of hydrogels on the surface of substrates. (d) Characterization of Gel 1 coated glass slide by SEM-EDS. Uncoated glass slide was characterized as a control. (e) Fluorescence images of uncoated and Gel 1 coated culture plates. The culture plates were incubated with *E. coli* expressing GFP.

can be explained by the yielding of hydrogen peroxide during the hydrolysis of $NaBO_3$ in aqueous solution. The TA/$NaBO_2$ hydrogels could be easily coated on substrates such as culture plates and glass slides due to the catechol groups on the gel surface (Fig. 3c). The SEM-EDS analysis in Fig. 3d suggests the successful coating of Gel 1 on a glass slide. After gel coating, the substrate effectively killed *E. coli* expressing green fluorescence protein (GFP, Fig. 3e). These results together suggest that the TA/borate gels have potent antibacterial activity.

We further expanded the gel responsiveness by using organic boronates to crosslink with TA. 1,4-Phenylenebisboronic acid (PBBA) with two boronate groups in the structure is expected to form catechol-boronate diesters for gelation (Fig. 4a) [21,22]. TA and PPBA formed stable gels within a high concentration ranges for both chemicals (Fig. 4b), and the yielding gel (Gel 5) is yellow-colored with G' higher than G'' in the rheology studies (Fig. 4c). PBBA showed a broad peak at 31.5 ppm in ^{11}B NMR, which is assigned to the trigonal-state of boronates on the chemical [37]. After the addition of TA, a new peak at 13.6 ppm is observed which is attributed to the formed catechol-boronate ester (Fig. 4d). The peak for catechol-boronate ester is disappeared in the presence of HCl, which is similar to the behavior of catechol-borate esters for Gel 1 and Gel 2 (Fig. 4e and Fig. S4 in Supporting information). Besides acid and base, the yielding gel is also responsive to oxidant chemicals such as H_2O_2, which is due to the oxidative degradation of PBBA into inorganic borates by H_2O_2 (Fig. 4e). This process is confirmed by the disappearance of the boronate ester peak in the ^{11}B NMR upon H_2O_2 addition (Fig. 4d). In comparison, the gels prepared by TA and $NaBO_2$ showed weak sensitivity to H_2O_2 under the same condition (Fig. 4e).

Finally, a commercially available organic boronate 4-mercaptophenylboronic acid (MPBA) was used as the boronate building block to prepare the dynamic covalent gels. MPBA was oxidized into dimers in the presence of DMSO and successfully formed a transparent gel with TA (Fig. 5a). ^{11}B NMR spectra suggested the formation of catechol-boronate esters in the mixture (Fig. 5b). The formed gel (Gel 6) responsiveness to acid, base, H_2O_2 (Fig. 5c and Fig. S5 in Supporting information), which is similar to Gel 5 in Fig. 4. Interestingly, Gel 6 also degraded rapidly in the presence of DTT, which is distinct from Gel 5. The DTT responsiveness of Gel 6 is explained by the cleavage of disulfide in the gel structure into thiol groups, which destroyed the crosslinking networks in the gel.

In summary, we reported a series of all-small-molecule dynamic covalent gels with antibacterial properties by direct gelation between TA and inorganic borates or organic boronates. In comparison with the responsive polymeric gels that require the pre-synthesis of macromolecular building blocks with chemical reactive ligands, the gels reported in this study are formed by direct gelation between natural occurring polyphenol TA and commercially available borate compounds. Besides facile construction, the all-small-molecule dynamic covalent hydrogels also show predictable degradation property. The hydrogels could be completely degraded into the small molecules upon multistimuli-responsiveness according to the chosen building blocks. The prepared dynamic covalent gels offer high flexibility to tune the physicochemical properties and responsiveness for various applications.

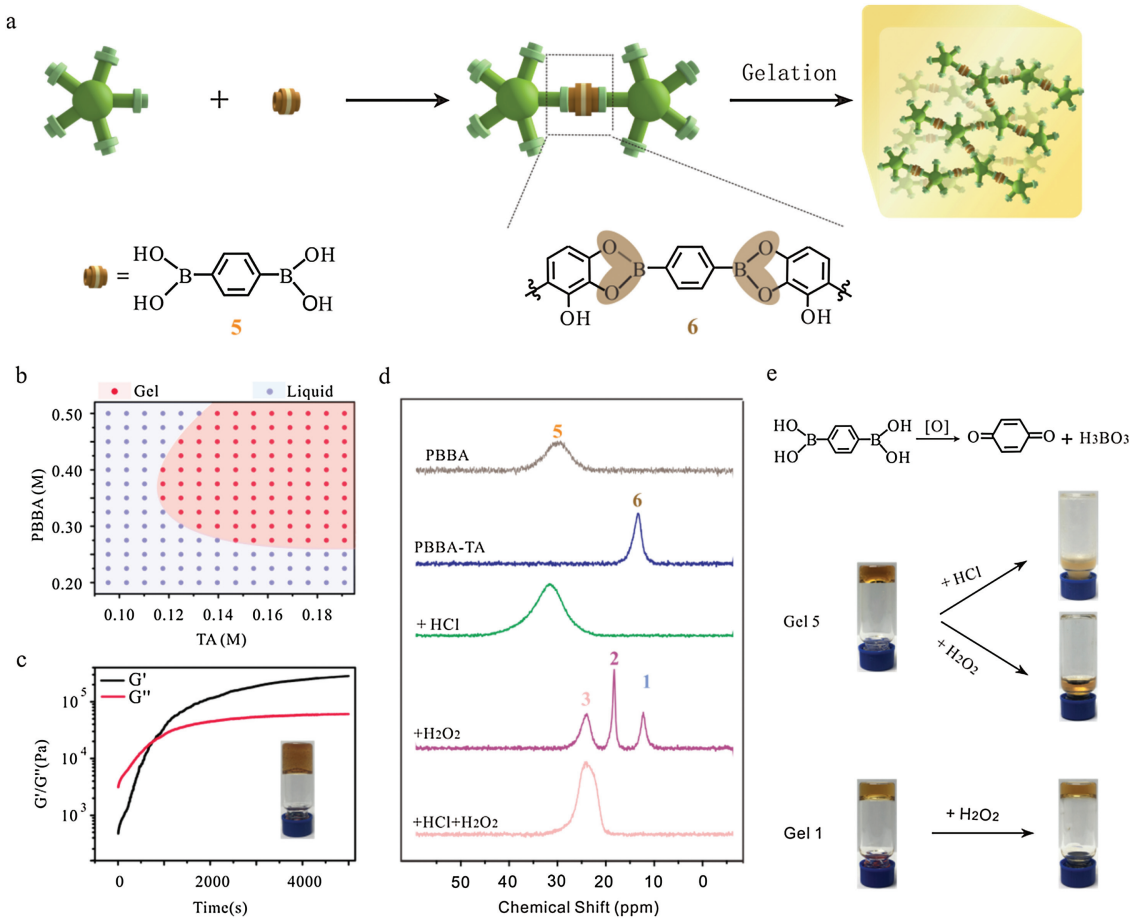

Fig. 4. (a) Formation of TA/PBBA gel by dynamic covalent connections. (b) Phase diagram of TA/PBBA mixtures. (c) Time-dependent rheology of the TA/PBBA (Gel 5). (d) ^{11}B NMR spectra of the TA/PBBA mixture in the presence of various triggers. (e) Acid- and H_2O_2-responsive behaviors of Gel 5. Gel 1 formed by TA and $NaBO_2$ is relatively stable in the presence of H_2O_2.

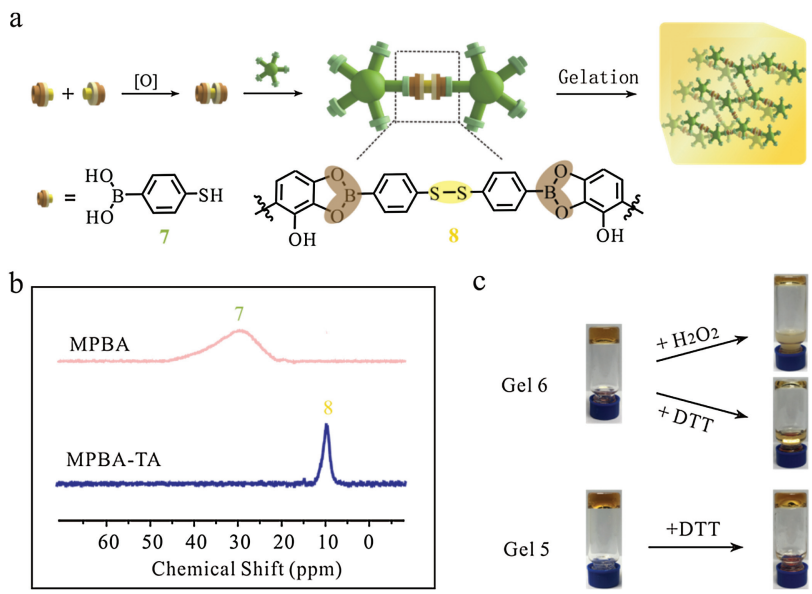

Fig. 5. (a) Concept of gelation between TA and MPBA. (b) ^{11}B NMR spectra of MPBA and TA/MPBA mixture. (c) H_2O_2- and DTT-responsive behaviors of the TA/MPBA gel (Gel 6). Gel 5 consisted of TA and PBBA is relatively stable in the presence of DTT.

Acknowledgements

This work is supported by the National Natural Science Foundation of China (No. 21725402) and the Shanghai Municipal Science and Technology Commission (No. 17XD1401600).

Appendix A. Supplementary data

Supplementary material related to this article can be found, in the online version, at doi:https://doi.org/10.1016/j.cclet.2019.07.013.

References

[1] Y. Shi, Z. Wang, X. Zhang, et al., Chem. Commun. 51 (2015) 15265–15267.
[2] D. Wang, Y. Hu, P. Liu, D. Luo, Acc. Chem. Res. 50 (2017) 733–739.
[3] W. Cao, X. Zhang, X. Miao, Z. Yang, H. Xu, Angew. Chem. Int. Ed. 52 (2013) 6233–6237.
[4] Z. Liu, T. Liu, Q. Lin, C. Bao, L. Zhu, Angew. Chem. Int. Ed. 54 (2015) 174–178.
[5] Z. Liu, Q. Lin, Y. Sun, et al., Adv. Mater. 26 (2014) 3912–3917.
[6] C.H. Fox, G.M. ter Hurrne, R.J. Wojtecki, et al., Nat. Commun. 6 (2015) 7417.
[7] J.M. Garcia, G.O. Jones, K. Virwani, et al., Science 344 (2014) 732–735.
[8] K. Iwaso, Y. Takashima, A. Harada, Nat. Chem. 8 (2016) 625–632.
[9] Y. Takashima, S. Hatanaka, M. Otsubo, et al., Nat. Commun. 3 (2012) 1270.
[10] J. Lou, F. Liu, C.D. Lindsay, et al., Adv. Mater. 30 (2018) 1705215.
[11] R. Tamate, K. Takahashi, T. Ueki, A.M. Akimoto, R. Yoshida, Biomacromolecules 18 (2017) 281–287.
[12] R. Guo, Q. Su, J. Zhang, et al., Biomacromolecules 18 (2017) 1356–1364.
[13] J.M. Poolman, J. Boekhoven, A. Besselink, et al., Nat. Protoc. 9 (2014) 977–988.
[14] G.M. Peters, L.P. Skala, T.N. Plank, et al., J. Am. Chem. Soc. 136 (2014) 12596–12599.
[15] G.M. Peters, L.P. Skala, T.N. Plank, et al., J. Am. Chem. Soc. 137 (2015) 5819–5827.
[16] J. Zheng, R. Fan, H. Wu, et al., Nat. Commun. 10 (2019) 1604.
[17] J.Y. Zhang, L.H. Zeng, J. Feng, Chin. Chem. Lett. 28 (2017) 168–183.
[18] M. Singh, S. Kundu, M.A. Reddy, et al., Nanoscale 6 (2014) 12849–12855.
[19] J.H. Lee, J. Park, J.W. Park, et al., Nat. Commun. 6 (2015) 6650.
[20] H. Wang, Y. Cheng, Mater. Chem. Front. 3 (2019) 472–475.
[21] S. Lamping, T. Otremba, B.J. Ravoo, Angew. Chem. Int. Ed. 57 (2018) 2474–2478.
[22] A.R. Narkar, B. Barker, M. Clisch, J. Jiang, B.P. Lee, Chem. Mater. 28 (2016) 5432–5439.
[23] J.V. Accardo, J.A. Kalow, Chem. Sci. 9 (2018) 5987–5993.
[24] Y. Chen, W. Wang, D. Wu, M. Nagao, D.G. Hall, Biomacromolecules 19 (2018) 596–605.
[25] T.T. Duncan, B.H. Berrie, R.G. Weiss, Appl. Mater. Interfaces 9 (2017) 28069–28078.
[26] M.E. Smithmyer, C.C. Deng, S.E. Cassel, et al., Macro. Lett. 7 (2018) 1105–1110.
[27] M.A. Rahim, M. Bjornmalm, T. Suma, et al., Angew. Chem. Int. Ed. 55 (2016) 13803–13807.
[28] J. Guo, B.L. Tardy, A.J. Christofferson, et al., Nat. Nanotechnol. 11 (2016) 1105–1111.
[29] J.H. Park, K. Kim, J. Lee, et al., Angew. Chem. Int. Ed. 53 (2014) 12420–12425.
[30] H. Fan, L. Wang, X. Feng, et al., Macromolecules 50 (2017) 666–676.
[31] M. Bishop, N. Shahid, J. Yang, A.R. Barron, Dalton Trans. (2004) 2621–2634.
[32] G.M. Peters, J.T. Davis, Supramol. Chem. 26 (2014) 286–295.
[33] Z. Liu, H. He, Acc. Chem. Res. 50 (2017) 2185–2193.
[34] A. Gennari, C. Gujral, E. Hohn, et al., Bioconjug. Chem. 28 (2017) 1391–1402.
[35] J.W. Tomsho, S.J. Benkovic, J. Org. Chem. 77 (2012) 2098–2106.
[36] M. Daglia, Curr. Opin. Biotechnol. 23 (2012) 174–181.
[37] M.L. Stolowitz, C. Ahlem, K.A. Hughes, et al., Bioconjug. Chem. 12 (2001) 229–239.